Proceedings of Ninth World Conference on Earthquake Engineering
August 2-9, 1988, Tokyo-Kyoto, JAPAN (Vol.III)

4-1-4

SHEAR MODULUS AND MATERIAL DAMPING OF DRY SAND UNDER TRUE TRIAXIAL STRESS STATES

Sheng-Huoo NI[1], Kenneth H. STOKOE, II[2] and José M. ROESSET[3]

[1]Associate Professor, Department of Civil Engineering, National Cheng-Kung University, Tainan, Taiwan, ROC
[2]Brunswick-Abernathy Regents Professor, Department of Civil Engineering, University of Texas at Austin, USA
[3]Paul D. and Betty Robertson Meek Centennial Professor, Department of Civil Engineering, University of Texas at Austin, USA

SUMMARY

The effect of true triaxial states of stress on the shear modulus and material damping of dry sand was investigated. Testing was performed with hollow specimens using a resonant column device. Testing was performed: 1. at shearing strains less than 0.001 percent, 2. over a range in principal stresses from 83 to 166 kPa (12 to 24 psi), and 3. with wave propagation always in a principal stress direction. Shear modulus and material damping were found to be affected mainly by the principal stresses in the directions of wave propagation and particle motion and to be nearly independent of the third principal stress.

INTRODUCTION

The effect of stress state on the stiffness in shear of the soil skeleton has recently been studied with both small-scale [Ref. 1] and large-scale [Refs. 2 and 3] triaxial devices. These studies resulted in the new finding that, when low-amplitude shear waves are propagated and polarized along principal stress directions, only stresses in the directions of wave propagation and particle motion affect the shear wave velocity (and hence shear modulus). Shear wave velocity is essentially unaffected by the third principal stress. Unfortunately, only small strains could be generated in these studies, and the effect of stress state on material damping could not be evaluated. Therefore, a triaxial resonant column has been developed with which larger strains can be generated (Ref. 4). In addition, the effect of true triaxial stress states on dynamic shear modulus and material damping ratio can be studied simultaneously. Results of tests with this equipment using dry sand are presented herein. Due to space limitations, only small-strain measurements are presented.

RESONANT COLUMN EQUIPMENT

Resonant column equipment used in this study is of the fixed-free type. In this configuration, the bottom of the soil specimen is rigidly fixed to the base while the top (free end) is connected to a drive system that is used to vibrate the specimen in torsional motion. The soil specimen has the shape of a right circular cylinder and may be solid or hollow. The basic operational principle is to excite the cylindrical specimen in first-mode torsional motion. Once the first mode is established, measurements are made of the resonant frequency, amplitude of vibration and free-vibration-decay curve. These measurements are then combined with equipment characteristics and specimen size to calculate shear wave velocity, shear modulus and shearing strain amplitude using elastic

theory. Material damping ratio is calculated from measurement of the free-vibration-decay curve by assuming a viscously damped, single-degree-of-freedom system.

A typical fixed-free resonant column device consists of an isotropic confinement system, height-change measurement system, drive system, and motion measurement system. However, several modifications were made for this study. First, a microcomputer was added so that data collection and reduction were completely automated. Second, the top cap and base pedestal were modified to permit hollow soil specimens to be subjected to true triaxial states of stress. This stress state was applied by loading each hollow specimen with an inner cell pressure which differed from the outer cell pressure while simultaneously applying an additional axial stress through a thin central wire. A simplified view of a hollow specimen is shown in Fig. 1. The central steel wire (diameter of 0.062 in. [1.6 mm]) was used so that boundary conditions independent of stress state remained essentially unchanged. The performance of the thin wire was verified by a series of analytical and experimental tests [Ref. 4].

SOIL SPECIMENS

The majority of the tests in this study were performed with a medium to fine, air-dried, washed mortar sand with a specific gravity of 2.67. For purposes of comparison, a limited number of tests were also performed with Reid-Bedford and Ticino sands. All three sands classify as SP in the Unified Soil Classification System. The average gradation curves are shown in Fig. 2.

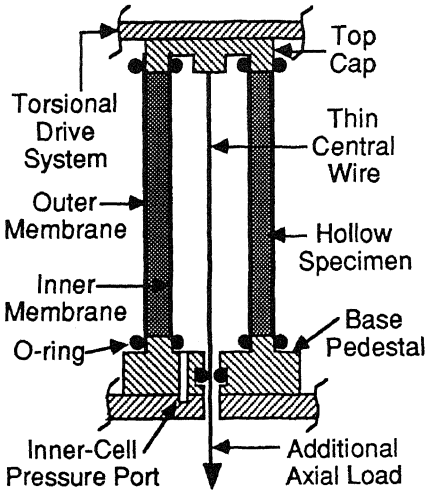

Fig. 1 Simplified Cross-Sectional View of Hollow Specimen

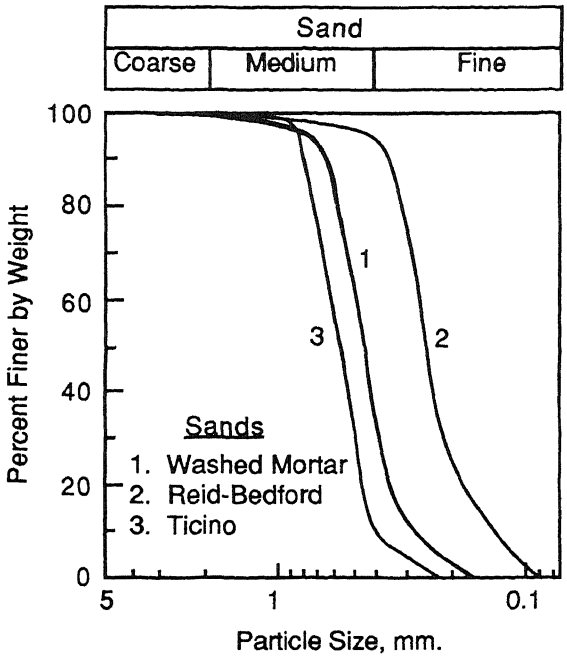

Fig. 2 Gradation Curves of Sands

Each hollow specimen was tested with nominal dimensions of: 36-mm (1.43-in.) inside diameter, 64-mm (2.5-in.) outside diameter and 142-mm (5.6-in.) height. Two split molds, inner and outer, were required to build the hollow specimens. The inside diameter of the hollow specimens was controlled by an inner split mold which was

covered by an inner membrane during construction. The inner split mold had a small gap which allowed the mold to collapse slightly upon withdrawal so that any friction between the inner mold and the inner membrane was nearly eliminated upon removal.

Each specimen was constructed in seven layers using the undercompaction method [Ref. 5]. The initial void ratios of all specimens ranged from 0.64 to 0.71. All three sands exhibited similar dynamic behavior. Therefore, only the results from four washed mortar specimens are presented. The void ratios of specimens 1, 2, 3 and 4 are 0.64, 0.65, 0.67 and 0.71, respectively.

STRESS NOTATION

The confining stresses applied to an element of soil during resonant column testing with true triaxial loading are shown in Fig. 3. The major principal effective stress, σ'_1, is applied in the vertical direction. This direction is also the direction of wave propagation, and the stress in this direction is denoted as σ'_a. The intermediate and minor principal effective stresses, σ'_2 and σ'_3, are applied in the circumferential and radial directions, respectively. Particle motion occurs in the circumferential direction, and the stress in this direction is denoted as σ'_b. The stress in the third direction, the radial direction, is called the out-of-plane stress and is denoted as σ'_c.

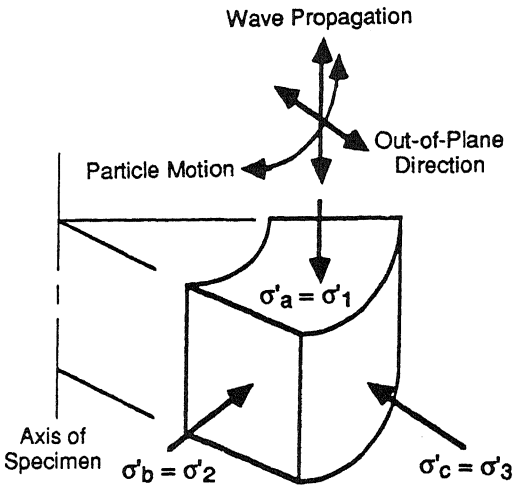

Fig. 3 Principal Stress Directions and and Associated Wave Motions

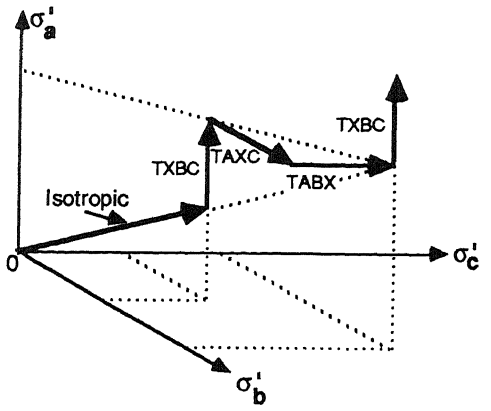

Fig. 4 Stage Loading Used in Applying True Triaxial Stresses

TEST PROCEDURE

Stage testing was employed in all low-amplitude tests, and measurements were performed after about 50 minutes of confinement at each stage. Low-amplitude tests are defined as those tests in which shearing strains did not exceed 0.001 percent. In true triaxial loading, stresses were varied independently by varying the vertical load, outer cell pressure and inner cell pressure independently. Due to the inherent nonuniformity in stresses in the σ'_b and σ'_c directions, average values of stresses were used for σ'_b and σ'_c. For convenience, the triaxial loading paths were classified as TXBC, TAXC or TABX as shown in Fig. 4. Capital letter T refers to a triaxial state of stress. The next three letters

in the notation refer to stresses in the σ'_a, σ'_b, and σ'_c, directions, respectively. Capital letters A, B or C mean that principal stresses σ'_a, σ'_b or σ'_c, respectively, were held constant during that loading stage. Capital letter X denotes the stress that was varied during that loading stage.

TEST RESULTS

At shearing strains less than 0.001 percent, the shear modulus and material damping ratio are essentially independent of strain amplitude and are commonly denoted as G_{max} and D_{min}, respectively. Therefore, measurements made at such small strains show the influence of only stress state (and any small variations between specimens due to void ratio variations).

The TXBC load path was used to investigate the effect of the principal stress in the direction of wave propagation on dynamic soil properties. Typical results of variations in G_{max} and D_{min} with axial stress are shown in Figs. 5a and 6a, respectively. The TAXC load path was used to investigate the effect of the principal stress in the direction of particle motion. Typical results of variations in G_{max} and D_{min} with lateral stress, σ'_b, are shown in Figs. 5b and 6b, respectively. Finally, the TABX load path was used to investigate the effect of the principal stress in the out-of-plane direction. Typical results of variations in G_{max} and D_{min} with lateral stress, σ'_c, are shown in Figs. 5c and 6c, respectively.

As shown in Figs. 5 and 6, the shear modulus of the sand was found to depend about equally on the principal stresses in the directions of wave propagation and particle motion and was determined to be nearly independent of the principal stresses in the out-of-plane direction. This behavior is best demonstrated by the log G_{max} - log σ'_a and log G_{max} - log σ'_b relationships which have essentially the same positive slopes (modulus increases with increasing stress) while the log G_{max} - log σ'_c relationship exhibits a slope of about zero. Material damping ratio was also found to depend about equally on the principal stresses in the directions of wave propagation and particle motion and was determined to be relatively independent of the principal stress in the out-of-plane direction. However, in contrast with G_{max}, D_{min} decreases with increasing stress, and no linear relationship between log D_{min} and log σ'_a or log σ'_b exists. Finally, for the same change in σ'_a or σ'_b, G_{max} exhibits a somewhat larger percentage change than D_{min}.

Another point to consider when evaluating the influence of triaxial stress state on shear modulus and material damping is that the general relationships can also be affected by stress ratio, K (= σ'_a/σ'_b) (Ref. 4). For values of stress ratio below about 2.5, the relationships shown in Figs. 5 and 6 hold. However, for values of K greater than 2.5, the log G_{max} - log σ'_a or log σ'_b relationship is no longer linear, and the log D_{min} - log σ'_a or log σ'_b relationship tends to increase with increasing stress. Therefore, one must also be aware of the magnitude of the stress ratio when assessing dynamic soil properties, and the discussion presented herein pertains to situations where stress ratios are below 2.5.

It is interesting to note that the results shown in Fig. 5 indicate that the typical procedure of relating dynamic shear modulus to the mean effective principal stress (Ref. 6) is not correct since the mean effective principal stress includes all three principal stresses. Low-amplitude shear modulus, G_{max}, can be expressed instead as:

$$G_{max} = \frac{S}{F(e)} \sigma'_a{}^{na} \sigma'_b{}^{nb} \sigma'_c{}^{nc} Pa^{1-na-nb-nc} \quad (1)$$

in which S = stiffness coefficient, F(e) = a function of void ratio (= 0.3 + 0.7 e^2), e = void ratio, na = slope of the log G_{max} - log σ'_a relationship, nb = slope of the log G_{max} - log σ'_b relationship, nc = slope of the log G_{max} - log σ'_c relationship, and Pa = atmospheric pressure. For the washed mortar sand, the average values are: S = 700, na = 0.22, nb = 0.20 and nc = 0.02. For all practical purposes, na and nb can be assumed to be equal (0.22) and nc can be assumed to be zero. The influence of triaxial stress state on G_{max} can then be plotted on one graph as shown in Fig. 7. For clarity, only a portion of the results are presented in Fig. 7.

CONCLUSIONS

Shear modulus and material damping of dry sand at small strains are shown to be affected mainly by the principal stresses in the directions of wave propagation and particle motion under true triaxial states of stress. The third principal stress exhibits very little influence on G_{max} or D_{min}. As a result, the mean effective stress is not the key stress component affecting G_{max} and D_{min} as is commonly assumed. In terms of the relationship between G_{max} and triaxial stress state, Eq. (1) which involves all three stress components most correctly describes this relationship. In addition, the stress ratio (σ'_a/σ'_b) can also affect the relationships between stress state and dynamic properties at stress ratios above about 2.5.

ACKNOWLEDGEMENTS

The authors would like to thank the United States Air Force Office of Scientific Research, Bolling Air Force Base, Washington, D.C. for sponsoring this research.

REFERENCES

1. Roesler, S.K. (1979), "Anisotropic Shear Modulus Due to Stress Anisotropy," Journal of the Geotechnical Engrg. Div., ASCE, Vol. 105, No. GT7, pp. 871-880.
2. Knox, D.P., Stokoe, K.H., II and Kopperman, S.E. (1982), "Effect of State of Stress on Velocity of Low-Amplitude Shear Waves Propagating along Principal Stress Directions in Dry Sand," Report GR82-23, University of Texas at Austin, 449 p.
3. Lee, S. H.-H. and Stokoe, K.H., II (1986), "Investigation of Low-Amplitude Shear Wave Velocity in Anisotropic Materials," Geotechnical Engineering Report GR86-6, University of Texas at Austin, 343 p.
4. Ni, T. S.-H. (1987), "Dynamic Properties of Sand Under True Triaxial Stress States from Resonant Column/Torsional Shear Tests," Ph.D. Dissertation, The University of Texas, Austin, Texas, 421 p.
5. Ladd, R.S. (1978), "Preparing Test Specimens Using Undercompaction," Geotechnical Testing Journal, ASTM, Vol. 1, No. 1, March, pp. 16-23.
6. Hardin, B.O. (1978), "The Nature of Stress-Strain Behavior for Soils," Proceedings, Geotechnical Engrg. Div. Specialty Conf. on Earthquake Engineering and Soil Dynamics, Vol. I, ASCE, Pasadena, California, June, pp. 3-90.

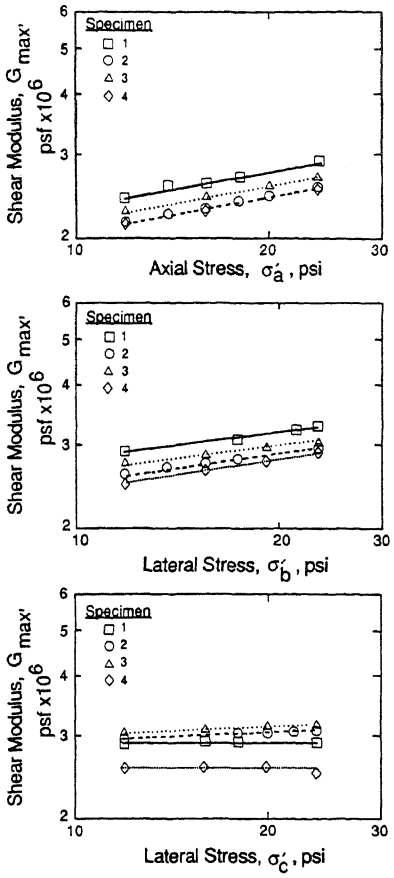

Fig. 5 Variation in G_{max} with σ'_a, σ'_b and σ'_c for TXBC, TAXC and TABX Load Paths, Respectively

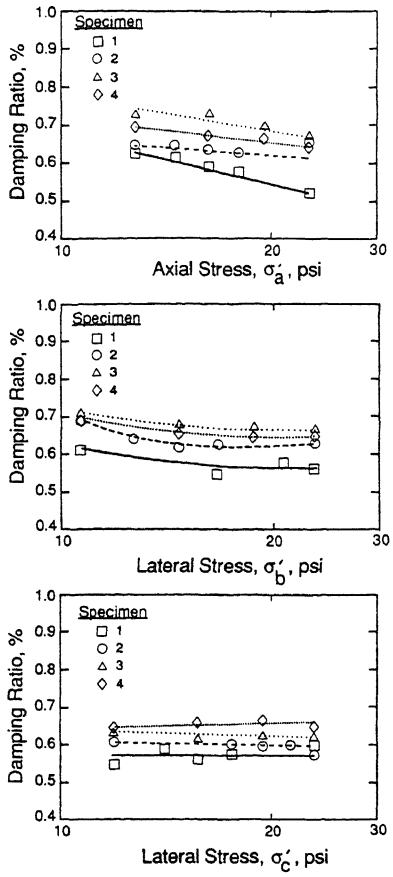

Fig. 6 Variation in D_{min} with σ'_a, σ'_b and σ'_c for TXBC, TAXC and TABX Load Paths, Respectively.

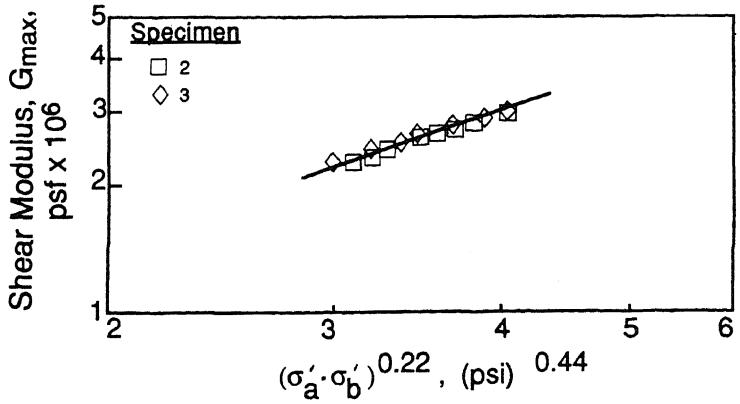

Fig. 7 Variation in G_{max} with Triaxial Stress State